Special Issue

Evaluating Polypoidal Choroidal Vasculopathy With Optical Coherence Tomography Angiography

Min Wang,[1,2] Yao Zhou,[1] Simon S. Gao,[3] Wei Liu,[1,2] Yongheng Huang,[1] David Huang,[3] and Yali Jia[3]

[1]Department of Ophthalmology and Vision Science, Eye and ENT Hospital, Fudan University, Shanghai, People's Republic of China
[2]Key Laboratory of Visual Impairment and Restoration of Shanghai, Shanghai, People's Republic of China
[3]Casey Eye Institute, Oregon Health & Science University, Portland, Oregon, United States

Correspondence: Min Wang, Department of Ophthalmology and Vision Science, Eye and ENT Hospital, Fudan University, Shanghai, People's Republic of China; wangmin83@yahoo.com.
Yali Jia, Casey Eye Institute, Oregon Health & Science University, Portland, OR 972239, USA; jiaya@ohsu.edu.

MW and YZ contributed equally to the work presented here and should therefore be regarded as equivalent authors.

Submitted: December 15, 2015
Accepted: June 19, 2016

Citation: Wang M, Zhou Y, Gao SS, et al. Evaluating polypoidal choroidal vasculopathy with optical coherence tomography angiography. *Invest Ophthalmol Vis Sci*. ;57:OCT526–OCT532. DOI:10.1167/iovs.15-18955

Purpose. We observed and analyzed the morphologic characteristics of polypoidal lesions and abnormal branching vascular network (BVN) in patients with polypoidal choroidal vasculopathy (PCV) by optical coherence tomography angiography (OCTA).

Methods. A retrospective observational case series was done of patients with PCV. All patients were scanned with a 70-kHz spectral-domain OCT system using the split-spectrum amplitude-decorrelation angiography (SSADA) algorithm to distinguish blood flow from static tissue. The OCTA images of these patients were compared to those from indocyanine green angiography (ICGA). Semiautomated segmentation was used to further analyze the polypoidal lesion and the BVN.

Results. We studied 13 eyes of 13 patients 51 to 69 years old. A total of 11 patients were treatment-naive. Two patients had multiple anti-VEGF injections and one underwent photodynamic therapy (PDT). Optical coherence tomography angiography was able to detect the BVN in all cases. Using cross-sectional OCTA, BVN locations were shown to be in the space between the RPE and Bruch's membrane. Using en face OCTA, the BVN vascular pattern could be shown more clearly than by ICGA. Polypoidal lesions showed high flow signals in different patterns in 12 cases in the outer retina slab. Using cross-sectional OCTA, the polyps were shown to be just below the top of the pigment epithelial detachment (PED). In one case, the polypoidal lesion was not detectable at the outer retina slab.

Conclusions. Optical coherence tomography angiography is a noninvasive imaging tool for detecting vascular changes in PCV. Branching vascular networks showed more clearly on OCTA than on ICGA. Polypoidal lesions had variable patterns on OCTA and were not always detected. The OCTA patterns of the polypoidal lesions and the BVN are helpful in understanding the pathology of PCV.

Keywords: optical coherence tomography angiography, polypoidal choroidal vasculopathy, branching vascular network

Polypoidal choroidal vasculopathy (PCV) was first reported by Yannuzzi et al.[1] as a distinct entity that clinically and demographically differs from neovascular age-related macular degeneration (nAMD). Compared to nAMD, patients with PCV are younger and more likely Asians, and eyes with PCV lack drusen, often manifest as serosanguinous maculopathy or hemorrhagic pigment epithelial detachment, and differ in responses to photodynamic therapy and anti-VEGF agents. However, they both have common environmental risk factors, such as smoking and hypertension.[2] Whether the PCV is a variant of nAMD or a specific idiopathic entity still is controversial.[3] Polypoidal choroidal vasculopathy is clinically characterized by polypoidal choroidal dilatations associated with an abnormal branching vascular network (BVN), while the nAMD was characterized by an abnormal choroidal neovascularization (CNV). Indocyanine green angiography (ICGA) is an important tool for diagnosing PCV.[4] However, ICGA requires intravenous dye injection, which is invasive. Although the incidence of adverse reactions to indocyanine green is low, and most of them were mild, they still occurred and even caused death.[5,6]

Optical coherence tomography provides typical findings of PCV, such as dome-shaped pigment epithelium detachment (PED) and a double-layer sign.[7] Optical coherence tomography angiography (OCTA) using a split-spectrum amplitude-decorrelation algorism (SSADA) allows us to noninvasively detect the blood flow in the retina and structural changes at the same time.[8] It has been reported that it could detect CNV in AMD and provides a useful approach for monitoring the CNV.[9–12] With this novel technology, we observed and analyzed the abnormal blood flow changes of the polypoidal lesion and BVN in patients with PCV.

Methods

Study participants were recruited from the Medical Retina Clinic at the Eye Ear Nose & Throat Hospital of Fudan University, Shanghai, from July 2014 to April 2016. This study

This work is licensed under a Creative Commons Attribution-NonCommercial-NoDerivatives 4.0 International License.

Table. Patients' Information Summary

Patient	Age, y	Sex	Eye	Treatment	Polyps in ICGA	Pattern of Polyps on OCTA	Pattern of BVN on OCTA
1	61	M	OS	No	1	Nodular	Medusa
2	53	F	OD	No	1	Ring	Tangle
3	51	M	OD	No	1	Ring	Feeder vessel
4	51	M	OS	No	1	Cluster	Tangle
5	69	M	OS	No	1	Cluster	Tangle
6	63	M	OD	No	1	Nodular	Seafan
7	62	M	OS	No	2	Nodular	Tangle
8	61	F	OD	No	1	Nodular	Tangle
9	54	M	OS	No	1	Ring	Tangle
10	58	M	OS	No	1	Ring	Tangle
11	59	M	OD	No	5	Dot	Tangle
12	65	M	OS	3 anti-VEGF+1PDT	1	Undetected	Tangle
13	64	M	OS	4 anti-VEGF+1PDT	1	Cluster	Tangle

was approved by the Institutional Review Board of EENT Hospital of Fudan University and informed consent was obtained from all participants. All investigations followed the tenets of the Declaration of Helsinki.

Patients with a large area of hemorrhage on the fundus or cloudy media that could significantly reduce the intensity of the OCTA signal were excluded. In this study, all PCV patients enrolled underwent a multimodal retinal imaging examination, including fundus photography, fluorescein angiography (FA), ICGA, spectral-domain optical coherence tomography (SD-OCT), and OCTA. Two retinal specialists (WM, LW) who were experienced in the assessment and management of PCV made the diagnosis of PCV.

Simultaneous FA and ICGA was performed with the Heidelberg Spectralis HRA+OCT (Heidelberg Engineering, Heidelberg, Germany). Real-time OCT combined with FA or ICGA was performed as well.

Optical coherence tomography angiography scans were performed using the RTVue-XR Avanti (Optovue, Inc., Fremont, CA, USA), a 70 kHz spectral-domain OCT system with a center wavelength of 840 nm. Each angiography scan consisted of one horizontal priority (*x*-fast) and one vertical priority (*y*-fast) raster scan. For each volumetric raster scan, there were 304 A-scans per B-scan, and two consecutive B-scans at 304 locations. Flow was detected using the SSADA algorithm.[8,13] Briefly, SSADA assesses the OCT reflectance variation on a voxel-by-voxel basis between two consecutive B-scans at each location via decorrelation to differentiate between flow (high decorrelation) and static tissue (low decorrelation). Split-spectrum processing of the OCT signal is used to improve the signal-to-noise ratio of flow detection. To correct for motion artifacts, the contained software registered and merged the *x*-fast and *y*-fast scans.[14]

Semiautomated segmentation was used to identify anatomic reference planes.[15] Maximum flow projection between the inner limiting membrane to inner (IPL) and outer (OPL) plexiform layers to Bruch's membrane produced en face angiograms of the superficial and outer retina, respectively. To create composite en face angiograms of the inner retina and neovascular membrane, the inner retina angiogram (purple) was overlaid on the expert grader contoured CNV (yellow). Composite cross-sectional B-scan images were created in a similar fashion by overlaying flow in the superficial and outer retina on structural OCT images.

Results

We studied 13 eyes of 13 patents 51 to 69 years old. Patient information is summarized in the Table. A total of 11 patients were treatment-naive. Two patient had multiple anti-VEGF injections and one underwent photodynamic therapy (PDT). In each case polyps and BVN were found on ICGA. The polypoidal lesion showed high flow signals in different patterns in 12 cases at the outer retina slab on OCTA. The polyps were located anatomically under the top of the PED. In one case, a polypoidal lesion was not detectable at the outer retinal slab. Optical coherence tomography angiography was able to detect the BVN in all cases. The patterns of the BVN on OCTA showed as seafan, medusa, and tangle. The BVN was located anatomically in the space between the RPE and Bruch's membrane on OCTA, and it showed clearer than on ICGA.

Case 1

In a 59-year-old male patient (patient 11 in the Table), the polypoidal lesions appeared as several orange-red lesions on fundus photography. Indocyanine green angiography in the early phase identified 5 typical polypoidal choroidal dilations. On structural OCT, the polypoidal lesion corresponded to the PED and the BVN corresponded to the double layer sign. On OCTA, the polypoidal lesions were detected as high flow signal spots in the left part of the BVN. The BVN showed clearer on OCTA than on ICGA. In the semiautomated segmentation, BVN showed as a high signal (yellow). On composite B scan, the blood flow signal of the BVN was in the space between the RPE and Bruch's membrane, and showed at lines 1 and 2. Both polyps and the BVN showed clearly on pseudo-color semiautomated segmentation.

Case 2

In a 58-year-old male patient (patient 10 in the Table), a large orange-red lesion showed on fundus photography. Indocyanine green angiography in the early phase identified a very obvious polypoidal choroidal lesion showing hyperfluorescence surrounded by a hypofluorescent pool and the BVN. Indocyanine green angiography combined with SD-OCT demonstrated that the polypoidal choroidal lesion and BVN on ICGA corresponded to the PED and double layer sign on SD-OCT. Optical coherence tomography angiography detected blood flow signals of the polyps and BVN. The semiautomated segmentation showed that the blood flow signals of polyps were under the top of the PED and those of the BVN were between the RPE and Bruch's membrane.

Discussion

Optical coherence tomography angiography is a noninvasive imaging technology for detecting the blood flow of PCV in a

Investigative Ophthalmology & Visual Science

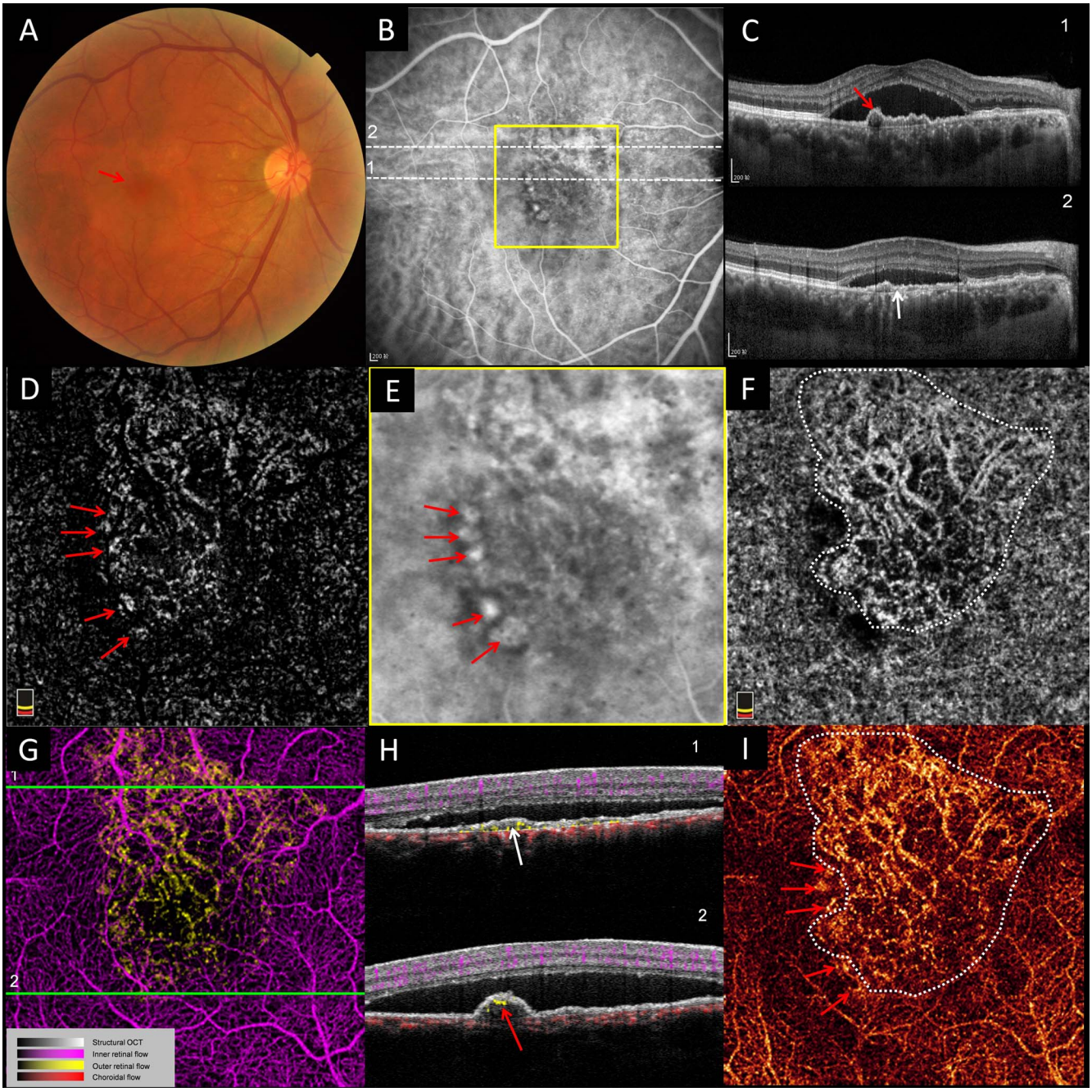

Figure 1. Multi-modal imaging of patient 11. (**A**) The fundus photograph shows orange-red polypoidal lesions (*red arrow*). (**B**) Early-phase ICGA shows polyps and BVN. (**C**) Spectral-domain OCT scans corresponding to the interrupted *white lines* in (**B**) identify PED (*red arrow*, cross-section 1 on *top*) and BVN (*white arrow*, cross-section 2 on *bottom*). (**D**) 3 × 3 mm macular en face OCTA of the outer retina reference. The high flow signal spots (*red arrow*) indicates the location of the polyps. (**E**) Enlarged ICGA (*yellow rectangle* in [**B**]) shows polyps (*red arrows*) and BVN. (**F**) 3 × 3 mm en face OCTA of the macula shows BVN (*white-dotted line enclosure*). (**G**) Color composite en face OCTA shows BVN flow (*yellow* outer retinal flow) in the context of normal retinal circulation (*purple* inner retinal flow). (**H**) Color composite cross-sectional OCTA shows that the BVN was in the space between RPE and Bruch's membrane (*white arrow*, cross-section 1 on *top*) and the polyps were just below the top of the PED (*red arrow*, cross-section 2 on *bottom*). (**I**) En face OCTA of the slab from outer boundary of OPL to BM shows polyps (*red arrows*) and BVN (*white dotted line enclosure*) clearly at the same time.

short testing time. We could obtain good quality OCTA images if the subject had relatively good fixation and clear media. We studied 13 cases of PCV with different manifestations on OCTA and ICGA.

From the OCTA findings of these 13 cases, a polypoidal lesion could be detected in 12 (92.3%) cases with the outer retinal slab. Kim et al.[16] mentioned that only 50% polyps were hyperreflective lesions on the outer retinal reference on OCTA. Inoue et al.[17] scanned patients with PCV and polypoidal CNV (PCNV), and found that the polyps flow within a focal point in the polypoidal lumen and that polyps were not clearly discernible on en face OCTA with the reference plane in the choroid capillary level. Srour et al.[18] indicated that 75% eyes with PCV showed a hypoflow round structure in correspon-

Investigative Ophthalmology & Visual Science

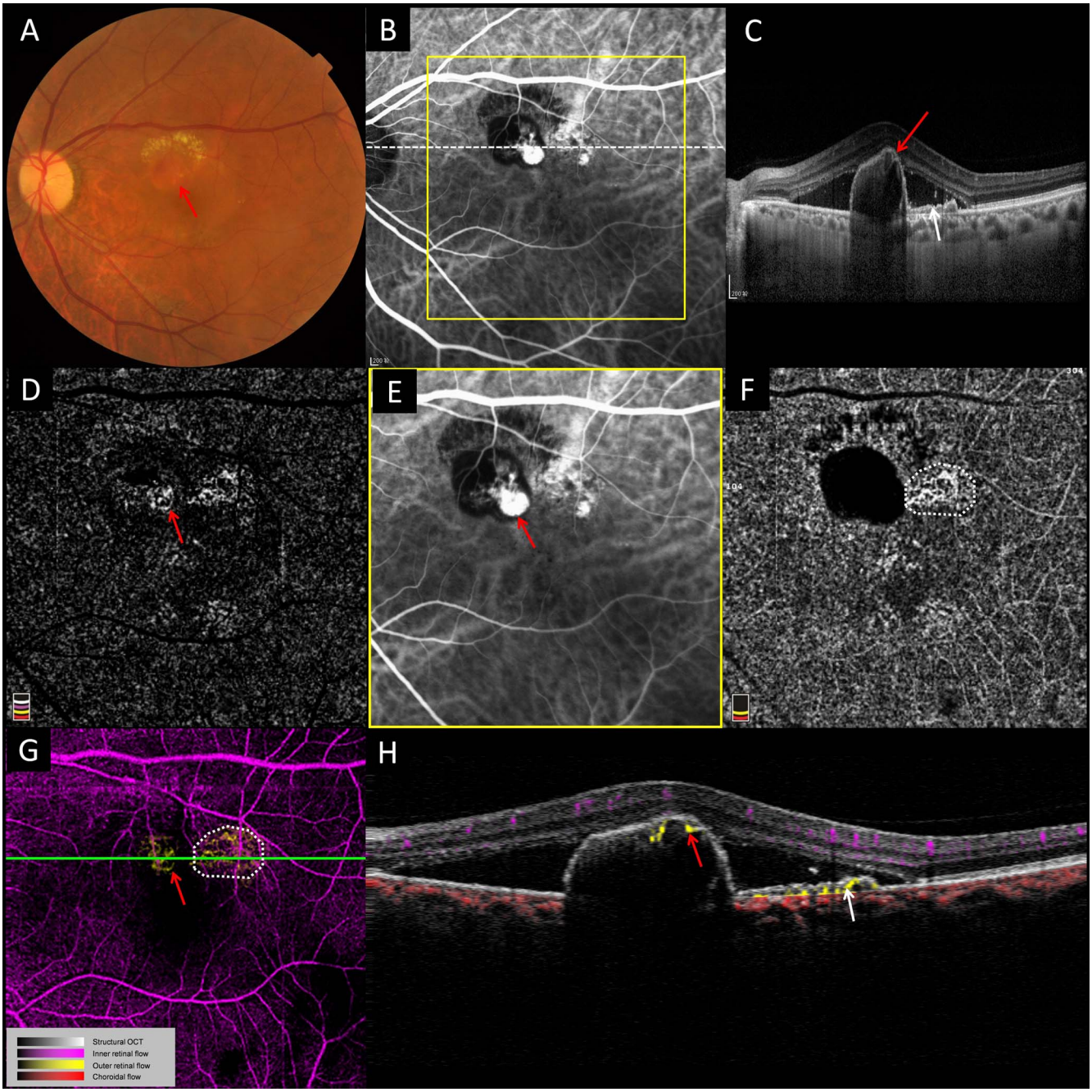

Figure 2. Multi-modal imaging of patient 10. (**A**) Fundus photography shows a large orange-red lesion (red arrow) (**B**) Early-phase ICGA shows the polyps as a hyper-fluorescent nodule surrounded by the hypo-fluorescent pool. The BVN is on the right side of the polyps. (**C**) The cross-sectional OCT crossing polyps (interrupted *white line* on [**B**]) identifies dome-shaped PED (*red arrow*) and BVN (*white arrow*). Hyperreflective signal under the *top* of PED can be observed. (**D**) 3 × 3 mm en face OCTA with the outer retina slab identifies the polyps (*red arrow*). The flow signals show as *white spots* with *half-circle*. (**E**) The *yellow rectangle* in (**B**) was enlarged for better comparison with OCTA. (**F**) 3 × 3 mm en face OCTA with the choroid capillary reference plane shows the BVN (*white-dotted line enclosure*). (**G**) Color composite en face OCTA identifies the polyps (*red arrow*) and BVN (*white-dotted line enclosure*). Signals of polyps show as high flow spots with a *half-circle*. (**H**) Color composite cross-sectional OCTA shows that the signals of polyps (*red arrow*) were just below the *top* of PED and the signals of the BVN (*white arrow*) were in the space between the RPE and Bruch's membrane.

dence with the polypoidal lesion on OCTA with segmentation of the choriocapillaris layer. Compared to the studies above, the polyp detection rate was higher in our study. Inoue et al.[17] and Srour et al.[18] all analyzed the signals of polyps on OCTA with the choroid capillary slab. This could miss some signals from the top of the PED, which is the location of the polyps. According to our experience, it would be better to choose the outer retina slab for observation of polyps on OCTA. The default en face display slab definitions of the outer retina are from 70 μm below the IPL to 30 μm below the RPE and the choroid capillary slab is from 30 to 60 μm below the RPE in the AngioVue software. Actually, in eyes with a detached RPE, the outer retina slab included the flow signal from the top of the detached RPE to Bruch's membrane.

Investigative Ophthalmology & Visual Science

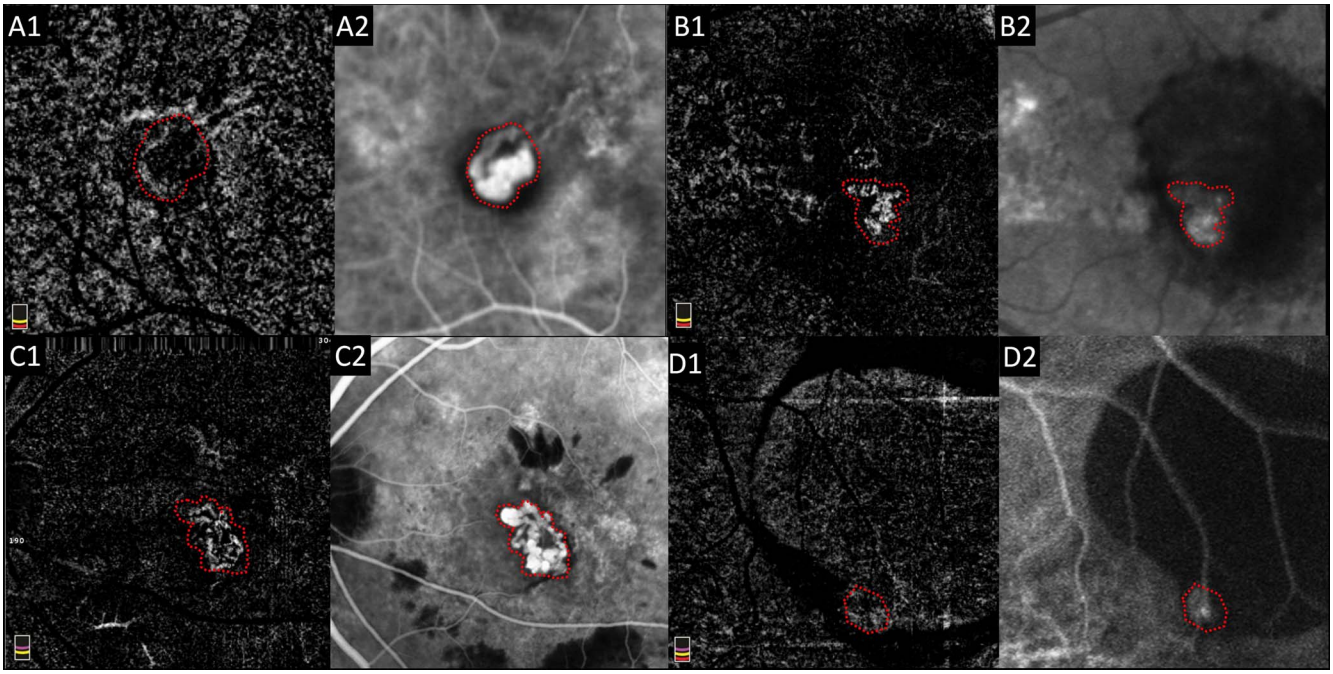

Figure 3. Comparison of the polyps with different vascular patterns by OCTA and ICGA. Optical coherence tomography angiography (**A1**) and ICGA (**A2**) of patient 3. Optical coherence tomography angiography with the outer retina slab shows the signals of the polyps as a circle (*red dotted line enclosure*). Early-phase ICGA shows a large hyperfluorescent nodule (*red dotted line enclosure*). Optical coherence tomography angiography (**B1**) and ICGA (**B2**) of patient 13. Optical coherence tomography angiography with the outer retina slab shows the signals of the polyps as some spots (*red dotted line enclosure*). Late phase ICGA shows corresponding polyps (*red dotted line enclosure*). Optical coherence tomography angiography (**C1**) and ICGA (**C2**) of patient 5. Optical coherence tomography angiography with the outer retina slab shows polyps as a cluster of high flow signals (*red dotted line enclosure*). Early-phase ICGA shows the corresponding polyps (*red dotted line enclosure*). Optical coherence tomography angiography (**D1**) and ICGA (**D2**) of patient 12. Optical coherence tomography angiography with the outer retina slab can not detect the flow signal at the location the polyps should be (*red dotted line enclosure*). Early-phase ICGA shows polyps as a hyperfluorescent spot (*red dotted line enclosure*).

Among these 12 cases, polypoidal lesions showed as different patterns, such as nodular, ring, dot, and cluster (Figs. 1, 2, 3). By comparing the en face OCTA of the polyps of patient 3 with the corresponding area on ICGA (Figs. 3A1, 3A2), we found that the obvious hyperfluorescence polyps on ICGA only showed a high flow signal as a ring at the periphery of the polypoidal lesion. The polyps of patient 3 manifested as a slow ICG filling by ICGA and this is not rare in PCV on ICGA,

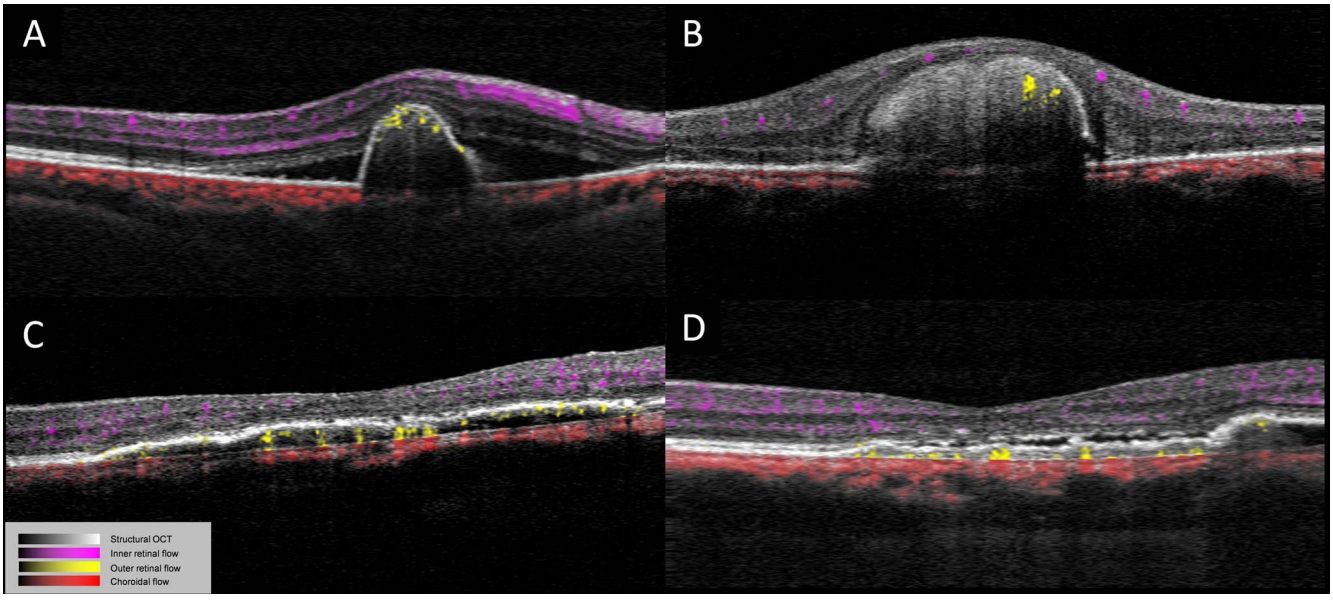

Figure 4. Color composite cross-sectional OCTA of four patients. Color composite cross-sectional OCTA of patients 2 (**A**) and 4 (**B**) show the signal of polyps (*yellow signals*). Signals of the polyps are just below the top of the PED (*red arrows*). Color composite cross-sectional OCTA of patients 12 (**C**) and 1 (**D**) show the signal of BVN (*yellow signals*). Signals of the BVN are in the space between the RPE and Bruch's membrane (*white arrows*).

Investigative Ophthalmology & Visual Science

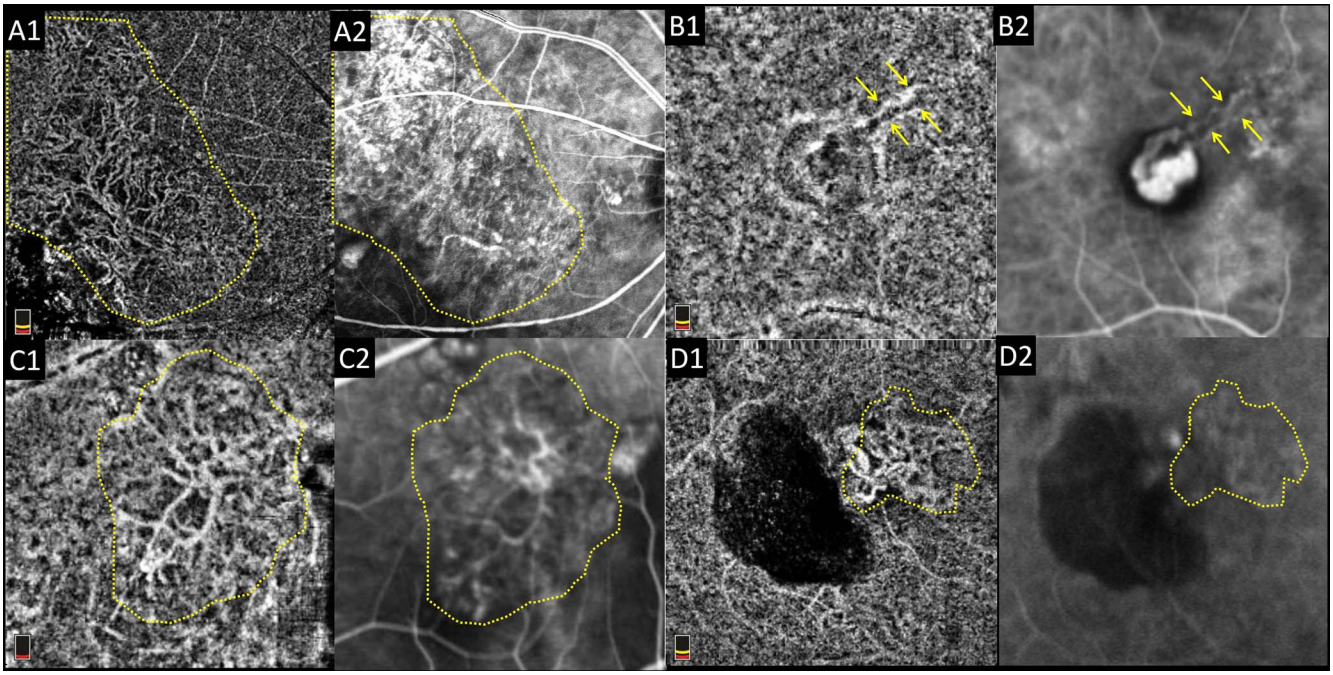

Figure 5. Comparison of the BVN with different vascular patterns by OCTA and ICGA. Optical coherence tomography angiography (**A1**) and ICGA (**A2**) from patient 6. Optical coherence tomography angiography with the choroid capillary slab shows the BVN with seafan pattern more clearly than ICGA (*yellow dotted line enclosure*). Early-phase ICGA shows the BVN (*yellow dotted line enclosure*). Optical coherence tomography angiography (**B1**) and ICGA (**B2**) from patient 3. Optical coherence tomography angiography with the choroid capillary slab shows feeder vessel and draining vessel (*yellow arrows*). Early-phase ICGA shows corresponding feeder vessel and draining vessel (*yellow arrows*). Polyps on ICGA shows more obvious than OCTA. Optical coherence tomography angiography (**C1**) and ICGA (**C2**) from patient 1. Optical coherence tomography angiography with the choroid capillary slab shows the BVN with medusa pattern more clearly than ICGA (*yellow dotted line enclosure*). Early-phase ICGA shows the BVN (*yellow dotted line enclosure*). Optical coherence tomography angiography (**D1**) and ICGA (**D2**) from case 8. Optical coherence tomography angiography with the choroid capillary slab shows the BVN with a tangle pattern more clearly than ICGA (*yellow dotted line enclosure*. Early-phase ICGA shows unclear BVN (*yellow dotted line enclosure*).

which probably is caused by the turbulence within the dilatation vessel.[19] According to the principal of SSADA, the slow velocity of the blood flow cannot be captured in OCTA due to the low decorrelation value[19] and the flow velocity at the periphery of this large polypoidal lesion could be faster than at the center, so OCTA captured the faster flow signals at the periphery and made them present as a ring. Sometimes the polypoidal lesion on ICGA was so small that the blood flow signal on OCTA was difficult to detect (Figs. 3D1, 3D2). Patient 12 had been treated with anti-VEGF injection and PDT. This could cause shrinkage of the polyps and difficulty in detecting them with OCTA. To the best of our knowledge, this is the first study to show the distinct blood flow changes inside the polyps with OCTA.

Color composite cross-sectional OCTA identified the polypoidal lesion beneath the top of the PED (Figs. 1H, 4A, 4B) Alshahrani et al.[20] summarized SD-OCT findings in 17 eyes with PCV and Khan et al.[21] analyzed 18 PCV cases with ICGA and OCT. They both demonstrated that the polyps were located in the sub-RPE space adherent to the posterior surface of the RPE. Their findings were very similar to our results of semiautomated segmentation.

Among our 13 patients, OCTA was able to detect the BVN in each case (100%) and the BVN showed more clearly on OCTA than on ICGA. The patterns of the BVN on OCTA included seafan, medusa, and tangle (Fig. 5). With color composite cross-sectional OCTA, the BVN flow signals were detected between the RPE and Bruch's membrane (Figs. 1H line 1, 4C, 4D), not in the inner choroid as previous literature suggested.[1] The patterns of the BVN on OCTA were very similar to type I CNV in wet AMD. Kuehlewein et al.[22] described the different patterns of type I CNV on OCTA in wet AMD as medusa and seafan, which were similar to the patterns of the BVN on OCTA in our study.

Our case series had several limitations. First, it was a small, retrospective cross-sectional case series. Second, we only selected typical cases of PCV. Third, the OCTA system did not allow us to customize the segmentation to follow the contour of the lesion in some cases. This could mislead interpretation of the OCTA image.

In conclusion, OCTA is a noninvasive imaging tool for detecting the blood flow changes in PCV. The different vascular pattern of BVN showed more clearly on OCTA than on ICGA. Optical coherence tomography angiography does not show the polyps as clearly as ICGA. The blood flow signal inside the polypoidal lesion showed a different pattern on OCTA because OCTA just does not image the entire polypoidal lesion as well as ICGA. The pattern of the flow signal of the polypoidal lesion and BVN on OCTA is helpful to better understand the pathology of PCV.

Acknowledgments

Supported in part by research grants from Shanghai Science and Technology Committee (14411965500), The Natural Science Foundation of Shanghai Municipal Science and Technology Commission (13ZR1406100), Shanghai Key Laboratory of Visual Impairment and Restoration, National Institutes of Health (NIH; Bethesda, MD, USA) Grants DP3 DK104397, R01EY024544, R01EY023285, P30 EY010572, and an unrestricted grant from Research to Prevent Blindness. Oregon Health & Science University (OHSU), David Huang and Yali Jia have a significant financial interest in Optovue, Inc. David Huang also has a financial

interest in Carl Zeiss Meditec, Inc. These potential conflicts of interest have been reviewed and managed by OHSU.

Disclosure: **M. Wang**, None; **Y. Zhou**, None; **S.S. Gao**, None; **W. Liu**, None; **Y. Huang**, None; **D. Huang**, Optovue, Inc. (F, I, R), P, Carl Zeiss Meditec, Inc. P; **Y. Jia**, Optovue, Inc. (F), P

References

1. Yannuzzi LA, Sorenson J, Spaide RF, et al. Idiopathic polypoidal choroidal vasculopathy (IPCV). *Retina*. 1990;10:1–8.
2. Kikuchi M, Nakamura M, Ishikawa K, et al. Elevated C-reactive protein levels in patients with polypoidal choroidal vasculopathy and patients with neovascular age-related macular degeneration. *Ophthalmology*. 2007;114:1722–1727.
3. Laude A, Cackett PD, Vithana EN, et al. Polypoidal choroidal vasculopathy and neovascular age-related macular degeneration: same or different disease? *Prog Retin Eye Res*. 2010;29:19–29.
4. Japanese Study Group of Polypoidal Choroidal Vasculopathy. Criteria for diagnosis of polypoidal choroidal vasculopathy [in Japanese]. *Nippon Ganka Gakkai Zasshi*. 2005;109:417–427.
5. Benya R, Quintana J, Brundage B. Adverse reactions to indocyanine green: a case report and a review of the literature. *Cathet Cardiovasc Diagn*. 1989;17:231–233.
6. Hope-Ross M, Yannuzzi LA, Gragoudas ES, et al. Adverse reactions due to indocyanine green. *Ophthalmology*. 1994;101:529–533.
7. Sato T, Kishi S, Watanabe G, Matsumoto H, Mukai R. Tomographic features of branching vascular networks in polypoidal choroidal vasculopathy. *Retina*. 2007;27:589–594.
8. Jia Y, Tan O, Tokayer J, et al. Split-spectrum amplitude-decorrelation angiography with optical coherence tomography. *Opt Express*. 2012;20:4710–4725.
9. Jia Y, Bailey ST, Wilson DJ, et al. Quantitative optical coherence tomography angiography of choroidal neovascularization in age-related macular degeneration. *Ophthalmology*. 2014;121:1435–1444.
10. El AA, Cohen SY, Semoun O, et al. Type2 neovascularization secondary to age-related macular degeneration imaged by optical coherence tomography angiography. *Retina*. 2015;35:2212–2218.
11. Huang D, Jia Y, Rispoli M, Tan O, Lumbroso B. Optical coherence tomography angiography of time course of choroidal neovascularization in response to anti-vascular treatment. *Retina*. 2015;35:2260–2264.
12. Lumbroso B, Rispoli M, Savastano MC. Longitudinal optical coherence tomography angiography study type 2 naïve choroidal neovascularization early response after treatment. *Retina*. 2015;35:2242–2251.
13. Gao SS, Liu G, Huang D, Jia Y. Optimization of the split-spectrum amplitude-decorrelation angiography algorithm on a spectral optical coherence tomography system. *Opt Lett*. 2015;40:2305–2308.
14. Kraus MF, Liu JJ, Schottenhamml J, et al. Quantitative 3D-OCT motion correction with tilt and illumination correction, robust similarity measure and regularization. *Biomed Opt Express*. 2014;5:2591–2613.
15. Tan O, Li G, Lu AT, Varma R, Huang D. Mapping of macular substructures with optical coherence tomography for glaucoma diagnosis. *Ophthalmology*. 2008;115:949–956.
16. Kim JY, Kwon OW, Oh HS, Kim SH, You YS. Optical coherence tomography angiography in patients with polypoidal choroidal vasculopathy [published online ahead of print November 30, 2015]. *Graefes Arch Clin Exp Ophthalmol*. doi:10.1007/s00417-015-3228-3.
17. Inoue M, Balaratnasingam C, Freund KB. Optical coherence tomography angiography of polypoidal choroidal vasculopathy and polypoidal choroidal neovascularization. *Retina*. 2015;35:2265–2274.
18. Srour M, Querques G, Semoun O, et al. Optical coherence tomography angiography characteristics of polypoidal choroidal vasculopathy [published online ahead of print February 2, 2016]. *Br J Ophthalmol*. doi:10.1136/bjophthalmol-2015-307892.
19. Yuzawa M, Mori R, Kawamura A. The origins of polypoidal choroidal vasculopathy. *Br J Ophthalmol*. 2005;89:602–607.
20. Alshahrani ST, Al SH, Kahtani ES, Ghazi NG. Spectral-domain optical coherence tomography findings in polypoidal choroidal vasculopathy suggest a type 1 neovascular growth pattern. *Clin Ophthalmol*. 2014;8:1689–1695.
21. Khan S, Engelbert M, Imamura Y, Freund KB. Polypoidal choroidal vasculopathy: simultaneous indocyanine green angiography and eye-tracked spectral domain optical coherence tomography findings. *Retina*. 2012;32:1057–1068.
22. Kuehlewein L, Bansal M, Lenis TL, et al. Optical coherence tomography angiography of type 1 neovascularization in age-related macular degeneration. *Am J Ophthalmol*. 2015;160:739–748.

Investigative Ophthalmology & Visual Science